Final Draft
of the original manuscript:

Esper, J.; Schneider, L.; Krusic, P.J.; Luterbacher, J.; Buentgen, U.;
Timonen, M.; Sirocko, F.; Zorita, E.:

European summer temperature response to annually dated volcanic eruptions over the past nine centuries

In: Bulletin of Volcanology (2013) Springer

DOI: 10.1007/s00445-013-0736-z

European summer temperature response to annually dated volcanic eruptions over the past nine centuries

Jan Esper[1,*], Lea Schneider[1], Paul J. Krusic[2], Jürg Luterbacher[3], Ulf Büntgen[4], Mauri Timonen[5], Frank Sirocko[6], Eduardo Zorita[7]

[1]*Department of Geography, Johannes Gutenberg University, 55099 Mainz, Germany*
[2]*Department of Physical Geography and Quaternary Geology, Stockholm University, 10691 Stockholm, Sweden*
[3]*Department of Geography, Climatology, Climate Dynamics and Climate Change, Justus-Liebig University, 35390 Giessen, Germany*
[4] *Swiss Federal Research Institute WSL, 8903 Birmensdorf, Switzerland*
[5]*Finnish Forest Research Institute, Rovaniemi Research Unit, 96301 Rovaniemi, Finland*
[6]*Institute for Geoscience, Johannes Gutenberg University, 55099 Mainz, Germany*
[7]*Institute for Coastal Research, HZG Research Centre, 21494 Geesthacht, Germany*

* Corresponding author
E-mail: esper@uni-mainz.de, Phone: +49 6131 3922296, Fax: +49 6131 3924735

Revision submitted to
Bulletin of Volcanology

Abstract

The drop in temperature following large volcanic eruptions has been identified as an important component of natural climate variability. However, due to the limited number of large eruptions that occurred during the period of instrumental observations, the precise amplitude of post-volcanic cooling is not well constrained. Here we present new evidence on summer temperature cooling over Europe in years following volcanic eruptions. We compile and analyze an updated network of tree-ring maximum latewood density chronologies, spanning the past nine centuries, and compare cooling signatures in this network with exceptionally long instrumental station records and state-of-the-art General Circulation Models. Results indicate post-volcanic June-August cooling is strongest in Northern Europe two years after an eruption (-0.52 ±0.05 °C), whereas in Central Europe the temperature response is smaller and occurs one year after an eruption (-0.18 ±0.07°C). We validate these estimates by comparison with the shorter instrumental network, and evaluate the statistical significance of post-volcanic summer temperature cooling in the context of natural climate variability over the past nine centuries. Finding no significant post-volcanic temperature cooling lasting longer than two years, our results question the ability of large eruptions to initiate long-term temperature changes through feedback mechanisms in the climate system. We discuss the implications of these findings with respect to the response seen in General Circulation Models and emphasize the importance of considering well-documented, annually dated, eruptions when assessing the significance of volcanic forcing on continental scale temperature variations.

Keywords Volcanic forcing, Tree-rings, Climate, Instrumental stations, Maximum latewood density, Europe

Introduction

Sulfate aerosols, from volcanic sulfur injected into the stratosphere by explosive eruptions, tend to cool global surface temperatures (Cole-Dai 2010). The aerosols scatter incoming solar radiation and absorb outgoing infrared radiation, thereby warming the lower stratosphere and cooling the earth's surface (Robock 2000). Explosive eruption plumes that pass the tropopause, where the temperature lapse rate reaches an abrupt minimum (~9-17 km asl.), cause large-scale changes in atmospheric optical depth and negative radiative forcing (McCormick et al. 1993). Eruptions of this size are typically classified as having a volcanic explosivity index (VEI) ≥ 5 (Newhall and Self 1982). The tephra volume of such eruptions is estimated to exceed one billion cubic meters.

Estimates of post-volcanic cooling are based on the analysis of surface temperatures following large eruptions (Self et al. 1981; Kelly and Sear 1984; Angell and Korshover 1985; Sear et al. 1987; Robock and Mao 1995). The number of VEI ≥ 5 eruptions captured within the modern instrumental period is small (n = 10, 1901-2012), thus limiting the confidence of estimates based solely on observational data. Estimating the degree of cooling by eruptions prior to the era of instrumental observation necessitates the use of annually resolved temperature proxies that explain a fraction of temperature variance of which only tree-ring, and a few documentary records, have the temporal precision and accuracy to provide adequate information over the past millennium (Frank et al. 2010). The suitability of tree-ring proxy data to detect the thermal signature of explosive eruptions, in space and time, has been successfully demonstrated (Briffa et al. 1998; Hegerl et al. 2003; Anchukaitis et al. 2012; Esper et al. 2013).

The Global Volcanism Program (GVP) has identified 37, annually dated, explosive eruptions in the Northern Hemisphere (NH) and tropics over the past 1000 years that likely injected

sulfate aerosols into the stratosphere (Siebert et al. 2010). Though caution is required when working with these data as some of the eruptions have been dated using tree-ring records, which can lead to a circular reasoning when combining tree-ring reconstructed cooling estimates with eruption histories derived from the same proxy data. In addition, the sulfur emission magnitude, as well as the plume altitude, vary among VEI classified eruptions. Alternatively, histories of explosive eruptions derived from sulfate deposition in Greenland and Antarctic ice cores (Crowley 2000; Gao et al. 2008; Crowley and Unterman 2012) can be used to assess post-volcanic cooling (Ammann et al. 2007). However, this approach is constrained by dating uncertainties of the ice core acid layers that increases back in time and limits the temporal precision of inferred post-volcanic cooling estimates (Hammer et al. 1986; Traufetter et al. 2004; Baillie 2010).

The amplitude and duration of post-volcanic surface cooling is not well constrained and recently received critical examination (Anchukaitis et al. 2012; Mann et al. 2012; Esper et al. 2013). Hemispheric scale estimates, derived from observational and annually resolved proxy data (mainly tree-rings), range from ~ 0.0 to -0.4°C (Mass and Portman 1989; Briffa et al. 1998; Jones et al. 2003; D'Arrigo et al. 2009). It has been shown that the cooling signal is stronger during the summer season and in high European latitudes compared to lower latitudes (Fischer et al. 2007; Hegerl et al. 2011). Previous work, utilizing temperature simulations from Energy Balance and Coupled General Circulation Models (CGCMs) indicate the frequency of stratospheric volcanic clouds may have triggered long-term temperature variations responsible for cold conditions during the Little Ice Age (LIA) in the seventeenth and early nineteenth centuries (Crowley 2000; Wagner and Zorita 2005; Hegerl et al. 2011). Other studies (Robock 2000; Grove 2001; Schneider et al. 2009; Miller et al. 2012) suggest the clustered volcanic eruptions in the thirteenth century, including the 1258/59 unknown event identified in ice core sulfuric acid depositions (Langway et al. 1988),

contributed to the transition from the Medieval Warm Period (MWP) to the LIA about 700 years ago (see also Timmreck et al. 2009), a period during which a global reorganization of climate has been suggested (Graham et al. 2007, 2011; Trouet et al. 2009). However, the ability of CGCM's to accurately capture the dynamical response to stratospheric volcanic clouds is not without its own controversy (Stenchikov et al. 2006; Anchukaitis et al. 2010, Zanchettin et al. 2013a,b). An analysis of the dynamic response by twelve Coupled Model Intercomparison Project 5 (CMIP5) simulations to a suite of eruptions from the instrumental period indicated the models consistently overestimate tropical troposphere cooling leading to unstable pressure fields over high latitudes in the NH (Driscoll et al. 2012).

Here we present estimates of post-volcanic cooling over Northern and Central Europe derived from an updated network of tree-ring maximum latewood density (MXD) records covering the past 900 years (Büntgen et al. 2010; Esper et al. 2012a). Tree-ring MXD is a superior parameter for studying the effects of volcanic eruptions – compared to the more commonly used tree-ring width (TRW) measurements – as it is not biased by biological memory effects that tend to smear and lengthen the inferred TRW response to distinct climatic disturbances (Frank et al. 2007). We compare the temperature response to 34 of 37, annually dated and documented, VEI $\geq$ 5 eruptions, found in the summer temperature sensitive MXD network to the response found in a network of shorter instrumental records back to 1722 C.E. We also perform two sensitivity tests with subsets of volcanic eruptions representing *(i)* different VEI intensities, and *(ii)* the latitude of eruptions. We relate our cooling estimates from annually dated eruptions documented by the GVP with estimates derived from volcanic sulfate peaks identified in ice core records. Finally, our best estimates of post-eruption cooling are related to the annual summer temperature variance from 1111-1976 C.E. to evaluate the statistical significance of volcanic forcing in the context of natural climate variability over the past nine centuries.

Material and Methods

GVP and ice core data

Thirty-four annually dated large eruptions (VEI ≥ 5) from the NH and (NH and SH) tropics that occurred between 1111-1976 C.E. were used for assessing post-volcanic cooling effects (Table 1). Three eruptions (1480, 1482, 1800) that met these criteria were not considered, as these events were dated using dendrochronological methods (Siebert et al. 2010). The 34 eruptions have been precisely dated through documentary evidence and exceed VEI 4 above which stratospheric production of sulfate aerosols is expected based on descriptions of eruption type, duration, and column height (Newhall and Self 1982). The estimated tephra ejecta of these eruptions range from 1 to 160 10^9 m^3 (Table 1).

In addition to the 34 VEI ≥ 5 events (SEA 1 in Table 1) subsets of eruptions were tested to evaluate the significance of an eruption's size and the volcano's location on observed cooling patterns. These subsets include *(i)* 15 eruptions within the shorter 1722-1976 period, covered by long instrumental temperature data (SEA 2), *(ii)* 22 eruptions ≥ 1.5 10^9 m^3 tephra volume, and 12 eruptions < 1.5 10^9 m^3 tephra volume (SEAs 3 and 4), and *(iii)* volcanoes located in the NH extratropics and tropics (SEAs 5 and 6). Note that the average tephra volume of the tropical volcanoes is much larger (18.8 10^9 m^3) than the extratropical volcanoes (3.7 10^9 m^3).

Finally, we considered a timeseries of sulfate aerosol layers derived from multiple Greenland and Antarctic ice cores (Gao et al. 2008) identifying 40 NH stratospheric events between 1111-1976 C.E. (SEA 7). This record contains a number of major eruptions that are not documented by the GVP, including the 1452/53 Kuwae and 1258/59 unknown events, but are

identified in sulfate depositions and tree-ring chronologies (LaMarche and Hirschboeck 1984; Gao et al. 2006; Salzer and Hughes 2007). Though these ice-core derived data are typically used to force CGCMs, the dating and location of a number of eruptions, particularly during the earlier part of the past 900 years, is not certain (Hammer et al. 1986; Baillie 2008, 2010; Plummer et al. 2012; Sigl et al. 2013). This condition might compromise the temporal precision of any post-volcanic, climate assessment using such data. Only nine of the 40 ice core derived eruptions identified in Gao et al. (2008) coincide with a documented VEI ≥ 5 event during the 1111-1976 C.E. period (Table 1).

Tree-ring maximum latewood density chronologies

Documentary and ice core derived volcanic events were used to assess pre- and post-eruption June-August (JJA) temperature deviations reconstructed from European MXD chronologies spanning the past 900 years. An MXD chronology is the mean of a collection of MXD measurement series belonging to individual trees growing in an ecologically homogeneous site (Cook and Kairiukstis 1990). Typically, two such measurement series, representing two radii of a stem, are procured from each tree. The raw MXD series (in g/cm^3) need to be detrended/standardized to remove level differences between biologically younger and older tree-rings, which possess slightly denser and lighter latewood, respectively (Schweingruber et al. 1978). This is done by fitting negative exponential curves (NegExp) to the individual measurement series (radii) and calculating ratios between the raw density measurements and the curve values (Cook and Kairiukstis 1990). The procedure removes non-climatic, tree age-related trends and emphasizes common variations.

To produce a millennium-length chronology, MXD radial patterns from living trees, which typically represent the most recent 200-400 years, are crossdated (Douglass 1920) with patterns from relict trees (Büntgen et al. 2011). In the case of the MXD dataset from Northern Scandinavia (Fig. 1, NSC), relict material was obtained from trees that fell some hundred years ago into shallow lakes in Finnish Lapland and were preserved (Esper et al. 2012b). In other chronologies used in this study (see below), living trees were combined with historical timbers from old buildings (e.g. the Lötschental, Switzerland; Büntgen et al. 2006) or dry-dead wood in talus (e.g. the Pyrenees, Spain; Büntgen et al. 2008). Latewood cell-wall growth in these cold environments is controlled by summer temperature (Moser et al. 2010), imprinting a common variance among all single MXD measurement series at a given site (Figs. 1b and c). The coherence among individual measurement series is typically higher in MXD compared to TRW data (Esper et al. 2010). The common signal strength of tree-ring chronologies is also controlled by the number of integrated measurement series, which varies among sites and typically decreases back in time (in Figs. 1 b and c: 114 series over the recent 1947-1976 C.E. and 34 series over the early 1111-1140 C.E. periods).

Seven NegExp detrended MXD site chronologies, from latitudinal and elevational treeline environments in Northern and Central Europe, were used to assess the spatial and temporal temperature patterns associated with large volcanic eruptions (Table 2). The site chronologies are composed of *Pinus sylvestris* from Central (JAE) and Northern Scandinavia (TOR, NSC), *Pinus uncinata* from the Pyrenees (PYR), and *Larix decidua* and *Picea abies* from the Alps (LAU, LOE, TIR). The average number of MXD measurement series, over the common period 1111-1976 C.E., varies considerably among these datasets ranging from 18 in TOR to 49 in NSC. The lag 1 autocorrelation, a measure of the temporal persistence in a timeseries, is < 0.38 in all MXD site chronologies matching the memory inherent to instrumental JJA temperature data from the European stations used in this study (see below).

The regional mean timeseries, MXD-north and MXD-central, were calculated by averaging all the northern and central site chronologies (Fig. 2). This consolidation is justified by the significantly high inter-site correlations among the three northern (r_{north} = 0.57) and the four central sites ($r_{central}$ = 0.46) over the common period 1111-1976 C.E. It is important to note that the northern *versus* central site chronologies share no common variance (see the grey curve in Fig. 2d centered at r = 0.03) reflecting the distinct climatic dipole structure that exists over Europe as a consequence of internal climate forcings (Barnston and Livezey 1987). Inter-site correlations also decrease back in time – particularly among the northern sites (see the blue curve in Fig. 2d) – likely due to declining sample sizes in the site chronologies. This latter feature points to a weaker climatic signal in the site chronologies and subsequent regional composites during the earliest centuries of the past millennium. Replication of the entire European MXD network declines from 426 measurement series in 1973 to 87 series in 1111 C.E. (Fig. 2c).

Instrumental temperature data and calibration of MXD records

The MXD site and regional chronologies were transformed into estimates of average JJA temperature variability by scaling (adjusting the mean and variance; Esper et al. 2005) each chronology against the average JJA temperature of the nearest grid point in the Crutem4 temperature dataset (Jones et al. 2012) over the common period 1901-1976 (Table 3). The correlations between MXD chronology and JJA temperatures, at their respective grid points, are lower in Central Europe (ranging from 0.31 to 0.61) than in Northern Europe (0.71 to 0.82), indicating an overall weaker inherent climate signal in the central portion of the network. This tendency is confirmed by the correlations, calculated over a much longer time

period (1722-1976), between the mean JJA temperatures recorded at the Stockholm and Uppsala stations and the northern MXD chronologies, to the corresponding correlations computed for Central European chronologies and the long Central England, De Bilt, and Berlin station records (see last column in Table 3; Table S1).

Comparison of the spatial patterns of MXD summer temperature signals (Fig. 3) and the spatial patterns of the long European station record's summer temperature signals (Fig. S1) reveals increasing distance between the proxy sites and station locations is an additional source of correlation decay. The significant correlations ($p < 0.05$) between the northern MXD data and the gridded temperature data are spatially more homogeneous, reaching southward to a line across Northern Germany towards Ukraine. The significant portions of the overall weaker and more heterogeneous patterns of the Central European MXD data are centered over the Alps reaching into the central Mediterranean and the Balkans. The spatial overlap between the correlation patterns of the central MXD sites and the long station records (Figs. 3 and S1) indicates that the distance between proxy and station data affects the correlation results over the long 1722-1976 period in Central Europe, which is particularly obvious for the Mediterranean PYR site (Tab. 3: $r_{Crutem4} = 0.40$; $r_{Stations} = 0.17$). A similar feature is seen in Northern Europe, where the JAE site correlates lower than the TOR and NSC sites with the nearest grid points, but correlates better than the far northern MXD sites (TOR, NSC) with the Uppsala and Stockholm stations located in southern Sweden. These spatial associations help explain the overall better fit between the MXD-north mean timeseries and the station derived mean timeseries (JJA-north; see Fig. S2), compared to the MXD-central mean timeseries *versus* the Central European station mean (JJA-central). As the distance between proxy and station locations in the central portion of the network is larger, and their association is weaker, somewhat less coherent results should be expected when

estimating post-volcanic cooling effects from the MXD-central and JJA-central data over the common 1722-1976 period.

Coupled general circulation models

In addition to the European MXD and long instrumental station records, we used four millennium-long JJA temperature histories simulated by three CGCMs for the assessment of post-volcanic cooling effects (Supplementary Material). CGCM runs are typically used to attribute the influence of natural and anthropogenic forcings on climate, including the effects of explosive volcanism (Schneider et al. 2009). The simulations considered here include two millennium-long runs of the ECHO-G model (denoted Erik1 and Erik2; Zorita et al. 2005), as well as combined runs of the Max-Planck-Institute Earth System Model Paleoclimate version (MPI-ESM-P) and the Community Climate System Model version 4 (CCSM4; Gent el al. 2011) downloaded from the CMIP5 archive (Taylor et al. 2012; Fernández-Donado et al. 2013).

We extracted and averaged the simulated temperatures from each model run at five grid points in the vicinity of the northern MXD and station sites to produce a composite, simulated, JJA timeseries (CGCM-north; Fig. S3). The same procedure was applied to the seven grid points in vicinity to the central MXD chronologies and their corresponding long central stations (CGCM-central). The model composites are later used for comparison with the proxy derived, volcanic cooling estimates from 1111-1976. Note the simulated temperatures correlate only weakly between the four model runs in Northern Europe ($R_{1111-1976} = 0.12$) and Central Europe ($R_{1111-1976} = 0.08$), possibly related to the limited geographical region and the varying external forcings used in each model. Whereas the CCSM4 run has

been forced with the aerosol deposition data from Gao et al. (2008), Erik1 and Erik2 were forced using eruption estimates from Crowley (2000), and MPI-ESM-P with estimates from Crowley et al. (2008). The simulated summer temperatures also indicate slightly differing long-term trends from 1722-1976, as compared to the JJA-north and JJA-central station means (Fig. S3).

Superposed epoch analysis (SEA)

To assess post-volcanic cooling, we used SEA (Panofsky and Brier 1958) with *(i)* the temperature-transformed MXD site chronologies and their regional means (MXD-north, MXD-central), *(ii)* the long instrumental station records and their means (JJA-north, JJA-central), and *(iii)* the simulated JJA temperatures of the four CGCM runs and their means (CGCM-north, CGCM-central). In this experiment, the five years before and after a volcanic eruption are analyzed. Instrumental JJA temperature measurements, and their MXD-based and CGCM estimates, are expressed as anomalies with respect to the mean of the five years preceding the eruptions (years -5 to -1). SEA is applied to the 34 annually dated VEI ≥ 5 events, documented by the GVP (Siebert et al. 2010), over the 1111-1976 C.E. period, as well as the five additional subsets of those eruptions (SEA2-6 in Table 1). We also considered 40 volcanic events derived from sulfate aerosol layers in Greenland and Antarctic ice cores (SEA 7) and those eruptions used in a previous NH, living-tree MXD study of cooling patterns by Briffa et al. (1998) (Supplementary Material).

Results

Analysis of millennial-length MXD chronologies revealed severe post-volcanic summer cooling in Northern Europe and a reduced, but temporally extended, response in Central Europe associated with 34, precisely located and dated, large eruptions between 1111-1976 C.E. (Fig. 4). Northern European JJA temperatures, in year 1 and year 2 after the volcanic events, are -0.28 and -0.52°C. The individual MXD site chronologies from Scandinavia indicate fairly homogeneous patterns in these years (see the thin curves in Fig. 4) with a spread about their mean departure as small as ±0.08 °C at lag +1 and ±0.05°C at lag +2. Summer temperatures in Northern Europe rebound to +0.25°C by the fourth post-volcanic year. Cooling in Central Europe lasts until the fourth post-volcanic year (minimum at lag +1 = -0.18°C) and gradually returns to +0.02°C in year five after eruptions. However, relative to the temperature variations prior to stratospheric events (years -5 to -1), only the post-volcanic response in Northern Europe appears exceptional. In Central Europe, the post-volcanic deviations do not differ significantly from the centralized pre-volcanic estimates.

The 1111-1976 C.E. MXD derived, SEA temperature estimates (Fig. 4a) are strikingly similar to those found in both the 1722-1976 MXD and 1722-1976 instrumental station records (Figs. 4b and c), though the spread of SEA temperatures over the shorter period that contains 15 eruptions is larger. In Northern Europe, the dominating feature is the strong cooling in the second post-volcanic year, followed by a dramatic warming (+0.93°C station data) in the fourth. A similar pattern is evident in Central Europe where the JJA-central cooling signal (minimum -0.22°C) in year +1 vanishes among the pre- and post-volcanic temperature variations. Differences between the Central European MXD and instrumental SEA patterns, especially the station's positive anomaly in the fourth post-eruption year, are likely related to *(i)* the varying spatial coverage of the central MXD and observational data (Figs. 3 and S1), *(ii)* the unexplained temperature variance in the proxy data (larger in Central Europe compared to Northern Europe; Table 3), and *(iii)* the reduced number of VEI $\geq$ 5 volcanic

events since 1722 C.E. (n = 15), producing larger uncertainties (e.g., increased variance of the Central European MXD site's response in Fig. 4b).

The SEA results reveal stronger post-volcanic responses to tropical eruptions as compared to NH events (Figs. 4d and e) over the past 900 years, but relatively minor differences as a consequence of eruption size (i.e., < 1.5 vs. ≥ 1.5 10^9 m^3 tephra volume; Supplementary Material). It remains unclear whether the increased tropical eruption signature is due to the volcano's location – and associated increased stratospheric transport (Trepte and Hitchman 1992) – or driven by eruption size, as the mean tephra volume of the low latitude events (18.8 10^9 m^3) is much larger than the high latitude events (3.7 10^9 m^3). Also varying sulfur contents might contribute to the differentiation between Tropical and NH eruptions.

The strong temperature cooling found in Northern Europe following VEI ≥ 5 eruptions diminishes if ice-core derived volcanic events (Gao et al. 2008) are considered in the SEA (Fig. 5; details in Fig. S4), pointing to the importance of utilizing annually dated eruption data when assessing post-volcanic effects. Of course, the simulated Northern European summer temperatures indicate severe post-volcanic cooling in response to the Gao et al. (2008) events, if the CGCM (here CCSM4) has been forced with the same aerosol injection estimates (Fig. S5). In this case, post-volcanic cooling is much larger in the regional CCSM4 output (-0.90°C and -0.80°C at lags +1 and +2) than the cooling seen in both the MXD and instrumental data. The overall variance among the four CGCMs considered in the SEAs is significantly high, compared to the proxy and observational data, pointing to the limited validity of simulated temperatures at the scale of continental Europe (Supplementary Material).

The assessment of post-volcanic cooling in the context of the full spectrum of summer temperature variance over the 1111-1976 C.E. (n = 866 years) and 1722-1976 C.E. (n = 255

353 years) periods indicates that only mean deviations at lag +2 in Northern Europe differ
354 significantly ($p < 0.05$; Mann–Whitney–Wilcoxon test) from the mean of all years (Fig. 6).
355 Temperature cooling in year 1 after the stratospheric event – the most striking signal found in
356 Central Europe – is not significantly different from the mean of all years, even if the overall
357 variance of summer temperatures is less in Central Europe compared to Northern Europe (see
358 the density functions in Fig. 6). Visualization of the annual temperature estimates
359 demonstrates that *(i)* a number of post-volcanic JJA anomalies are actually positive (i.e., on
360 the right side of the centered distributions), and *(ii)* there are frequent cool years that are not
361 associated with stratospheric volcanic events. The latter finding is likely constrained by the
362 incompleteness of the volcanic record particularly during the earlier centuries of the past 900
363 years, albeit this argument is not valid for the shorter 1722-1976 C.E. period. The positive
364 deviations point to the importance of "unforced" internal variability of the climate system at
365 the European scale (Jungclaus et al. 2010).
366
367
368 **Discussion and Conclusions**
369
370 The analysis of an MXD network covering the past 900 years, and comparison with long
371 instrumental records since 1722 C.E., revealed severe summer temperature cooling two years
372 after stratospheric volcanic clouds in Northern Europe and a generally weaker response in
373 Central Europe. This spatial pattern supports findings based on a compilation of shorter proxy
374 and instrumental records (including documentary evidence) in response to selected tropical
375 eruptions (Fischer et al. 2007). However, the thermal cooling reported here, based on a
376 complete set of annually dated VEI ≥ 5 eruptions from the NH extratropics and tropics, is
377 weaker than that reported in Fischer et al. (2007) and, in Northern Europe, delayed by one
378 year (lag +2 instead of lag +1). Tests with respect to *(i)* eruption size (1–1.5 vs. $\geq 1.5\ 10^9\ m^3$

tephra volume), *(ii)* volcano location (NH vs. tropics), *(iii)* time period (1111-1976 vs. 1722-1976 C.E.), and *(iv)* volcanic forcing data (documentary vs. ice core reconstructed) demonstrate sensitivity of the cooling estimates to the selection criterion of eruptions. The marginal post-volcanic signals in both the Northern European MXD data and the long instrumental station data, in response to ice core derived sulfate deposition signatures (Gao et al. 2008), suggests caution should be used when considering these volcanic forcing estimates in CGCM studies (Solomon et al. 2007).

Documented *versus* ice core reconstructed volcanic histories

The documented and annually dated eruption data used here for the assessment of post-volcanic cooling indicates a higher frequency of stratospheric events during the more recent centuries of the past 900 years. There is a noticeable reduction of VEI ≥ 5 eruptions before 1450 C.E. (n = 2 events; Table 1), likely caused by incomplete documentary evidence from sparsely populated regions prior to the 16th century. During this early period a number of major volcanic events, including the 1258/59 unknown (Zielinski 1995) and 1452/53 Kuwae eruptions (Hammer et al. 1980; Sigl et al. 2013), have been identified in ice core acid layers from Greenland and Antarctica (Oppenheimer 2003; Kurbatov et al. 2006). These events are represented in the Gao et al. (2008) sulfate aerosol injection estimates used here for comparison of regional scale cooling effects. However, throughout the 1111-1976 C.E. period, only nine of the 40 NH and tropical stratospheric events included in Gao et al. (2008) match the annually dated VEI ≥ 5 events recognized by the GVP (Siebert et al. 2010).

The conclusion from these cooling estimates, based on documented *versus* ice core reconstructed volcanic histories, is somewhat ambivalent. The potentially missing

stratospheric events during earlier centuries of the past 900 years suggests cooling estimates from documented eruptions are too small, yet the substantially reduced Northern European cooling obtained from the ice core derived events contradicts this qualification. This conflicting result is likely related to dating uncertainties inherent to the ice core data (Hammer et al.1986; Robock and Free 1995) biasing the SEA-derived cooling estimates towards smaller deviations. Such an interpretation is supported by recent analyses of ice cores from high accumulation sites, questioning the dating of major volcanic events, including the 1452/53 Kuwae eruption (Plummer et al. 2012; Sigl et al. 2013) and challenging the common practice of using particular sulfuric acid layers as markers (e.g. 1258/59; Langway et al. 1988) to align stratigraphy between drill sites (Baillie 2008, 2010). The MXD network analyzed here indicates there were severe cooling events in 1453 C.E. in Northern Europe (coldest year of the past 900 years; labeled in Fig. 2) and 1258 C.E. in Central Europe (fourth coldest year; see also Fig. S6). The distinct cooling pattern identified at lag +2 in Northern Europe aggregated over 34 annually dated VEI $\geq$ 5 eruptions, implies the eruption associated with 1453 C.E. cooling even occurred as early as 1451 C.E. Admittedly, this inference is constrained by the limited geographical region (Northern Europe) represented by the MXD network in this study (Fig. 3) and the particular response to any single eruption as opposed to the overall mean signal.

Post-volcanic temperature patterns

The northern European cooling pattern reported here appears particularly robust, as the regional MXD data share a high degree of common variance and contain a strong climate signal (64% of MXD-north variance explained by JJA temperatures). The similarity between the SEA results derived from the northern MXD data over the past 900 years, and the

northern European instrumental data over the past 260 years, aids the detection of a volcanic signal two years after an eruption. The signal is likely associated with a positive (negative) sea level pressure and 500 hPa geopotential height anomaly over the central North Atlantic (eastern Scandinavia), connected to anomalous northwesterly and northerly flows towards central Europe (Fischer et al. 2007), suggesting a dynamical response to sub-continental cooling exists.

The high latitude post-volcanic cooling found here is much stronger than the signal reported by Briffa et al. (1998) for the NH extratropics (-0.11°C at lag +1), based on an analysis of a large-scale MXD network in response to 31 selected eruptions over the past 600 years (Fig. S4d). The Briffa et al. (1998) experiment, which also included MXD data from low latitude sites, produces an even weaker response (-0.08°C at lag +1 and -0.07 at lag +2) when strictly considering the annually dated NH and tropical VEI $\geq$ 5 eruptions since 1400 C.E. (SEA 1 in Table 1; n = 27 events). The much smaller temperature deviations in the Briffa et al. (1998) NH extratropical MXD network, compared to our findings from Europe, suggest spatially heterogeneous temperature patterns mitigate post-volcanic effects at the hemispheric scale.

Significance of cooling estimates

In Central Europe the lower coherence among MXD sites, as well as the weaker climate signal of the central portion of the network (27% of MXD-central variance explained by JJA temperatures), may bias the post-volcanic estimates towards reduced deviations, thereby affecting the statistical evaluation of significant cooling events with respect to the full spectrum of reconstructed summer temperature variability (Fig. 6). On the other hand, the weak post-volcanic signal seen in the central MXD data over the past 900 years is also found

in the long instrumental station records over the past 260 years suggesting a lower summer temperature sensitivity to stratospheric volcanic clouds in Central Europe. The similar temperature patterns found in the MXD based and instrumentally based SEAs indicates that those factors which could potentially bias the MXD network response, including enhanced tree growth due to increased diffuse light in post-volcanic years (Farquhar and Roderick 2003), are negligible (see also Krakauer and Randerson 2003). Our findings indicate that the prominent cooling following Tambora in 1816 C.E. (the "year without a summer"; Stothers 1984), as well as in 1912 C.E. (perhaps Novarupta), resulted from stratospheric volcanic clouds that caused atypical summer cooling over Central Europe.

It is important to note that the post-volcanic cooling estimates presented here are spatially restricted to Europe and cannot be transferred to global or even hemispheric dimensions. At this limited continental scale the density, length and quality of both the MXD network and long instrumental station data is unique, enabling assessments of cooling effects based on an exceptionally large number of stratospheric events (34 over the 1111-1976 C.E., and 15 over the 1722-1976 C.E. period). The key finding derived from this condition suggests the relaxation time of eruption induced climate anomalies to be on the order of at most a few years. This finding questions how large volcanic eruptions might initiate decadal, or even centennial scale, temperature changes through feedback mechanisms in the climate system (Crowley 2000; Robock 2000; Grove 2001; Schneider et al. 2009). While the temporally limited climate response, together with the reduced sensitivity found in response to ice-core derived forcing timeseries, belies the ability of large volcanic eruptions to initiate long-term temperature changes through feedback mechanisms in the climate system, there may be longer relaxation times in other systems – e.g. sea ice (Miller et al. 2012) and ocean temperatures (Church et al. 2005, Gleckler et al. 2006).

This conclusion is supported by the significance of observed, post-volcanic cooling with respect to the full spectrum of summer temperature variability found over the past 900 and 260 years. Figure 6 shows only the lag +2 cooling events in Northern Europe deviate at the 95% level from the mean summer temperature of all years over these periods. In Central Europe, the maximum likelihood of post-volcanic temperature cooling reaches approximately 80-85% (JJA-central over the 1722-1976 C.E. period at lag +1). Further research on *(i)* the dating uncertainty of eruptions, particularly during the MWP-LIA transition period (Esper et al. 2002) during which a global reorganization of climate has been suggested (Graham et al. 2007), as well as *(ii)* the development of millennial scale MXD records, that are less biased by biological memory effects than TRW records (Frank et al. 2007, Esper et al. 2007a), is needed to assess the ability of stratospheric volcanic clouds to trigger long-term temperature changes.

Eruption selection schemes

Besides the length of skillful temperature reconstructions, the identification and selection of eruption years appears relevant when assessing post-volcanic cooling effects. Consideration of invariable selection criteria (e.g. tephra volume > 1.0 10^9 m^3) seems advisable, particularly if the period covered by the temperature reconstructions, and thereby the number of volcanic events, is limited. SEA results based on just a dozen eruptions will be sensitive to the inclusion or exclusion of single events, e.g. inclusion of a certain VEI 5 (or even VEI 4) event but exclusion of another VEI 5 event, for example. Similarly, inclusion of selected dendro-dated or ice-core derived events – or temporal shifting of the ice core data to match the temperature proxies – is not recommended as such procedures would likely advance inflated post-volcanic cooling estimates. The approach used here, considering only the annually dated events exceeding a pre-defined VEI threshold, is again constrained by differing sulfur

emission magnitudes and eruption plume altitudes. These climatically important measures vary considerably among the VEI = 5 eruptions, for example.

The results shown here using state-of-the-art CGCMs suggest consideration of simulated post-volcanic cooling estimates, as a guideline for empirically based estimates, is not advisable at the sub-continental scale. The simulated summer temperatures over Central and Northern Europe do not cohere among the models, a finding that is largely controlled by the differing volcanic histories used to force the models. As expected, the simulated post-volcanic cooling effects appear much larger if the CGCM runs are aligned by the exact same volcanic events used to force the models. In addition, differences in the models innate climate dynamics, as well as the limited geographical region (grid points in Central and Northern Europe) likely contribute to the inconsistency among the simulations.

Acknowledgements

Supported by the Mainz Geocycles Research Centre. J.L. acknowledges support from the EU/FP7 project ACQWA (NO212250), the DFG Projects PRIME 2 (`PRecipitation In past Millennia in Europe- extension back to Roman times') within the Priority Program `INTERDYNAMIK' and `Historical climatology of the Middle East based on Arabic sources back to ad 800'.

References

Ammann CM, Joos F, Schimel DS, Otto-Bliesner BL, Tomas RA (2007) Solar influence on climate during the past millennium: Results from transient simulations with the NCAR Climate System Model. Proc Nat Acad Sci 104:3713–3718

Anchukaitis KJ, Buckley BM, Cook ER, Cook BI, D'Arrigo RD, Ammann CM (2010) The influence of volcanic eruptions on the climate of the Asian monsoon region. Geophys Res Lett 37. doi:10.1029/2010GL044843

Anchukaitis KJ, et al. (2012) Tree rings and volcanic cooling. Nature Geosc 5:836–837

Angell JK, Korshover J (1985) Surface temperature changes following the six major volcanic episodes between 1780 and 1980. J Clim Appl Meteorol 24:937–951

Baillie MGL (2010) Volcanoes, ice-cores and tree-rings: one story or two? Antiquity 84:202–215

Baillie MGL (2008) Proposed re-dating of the European ice core chronology by seven years prior to the 7th century AD. Geophys Res Lett 35. doi:10.1029/2008GL034755

Barnston AG, Livezey RE (1987) Classification, seasonality and persistence of low-frequency atmospheric circulation patterns. Mon Wea Rev 115:1083–1126

Briffa KR, Jones PD, Schweingruber FH, Osborn TJ (1998) Influence of volcanic eruptions on Northern Hemisphere summer temperature over the past 600 years. Nature 393:450–455

Büntgen U, Frank DC, Nievergelt D, Esper J (2006) Summer temperature variations in the European Alps, AD 755–2004. J Clim 19:5606–5623

Büntgen U, Frank DC, Grudd H, Esper J (2008) Long-term summer temperature variations in the Pyrenees. Clim Dyn 31:615–631

Büntgen U, Frank D, Trouet V, Esper J (2010) Diverse climate sensitivity of Mediterranean tree-ring width and density. Trees 24:261–273

Büntgen U, et al. (2011) European climate variability and human susceptibility over the past 2500 years. Science 331:578–582

Church J, White N, Arblaster JM (2005) Significant decadal-scale impact of volcanic eruptions on sea level and ocean heart content. Nature 438:74–77

Cole-Dai J (2010) Volcanoes and climate. WIREs Clim Change 1:824–839

559 Cook ER, Kairiukstis, LA (eds) (1990) Methods of dendrochronology: applications in
560 environmental science. Kluwer, Dordrecht

561 Crowley TJ (2000) Causes of climate change over the past 1000 years. Science 289:270–277

562 Crowley T, Zielinski G, Vinther B, Udisti R, Kreutz K, Cole-Dai J, Castellano E (2008)
563 Volcanism and the Little Ice Age. PAGES Newsletter 16:22-23

564 Crowley TJ, Unterman MB (2012) Technical details concerning development of a 1200-yr
565 proxy index for global volcanism. Earth Syst Sci Data Discuss 5:1–28

566 D'Arrigo R, Wilson R, Tudhope A (2009) Impact of volcanic forcing on tropical temperatures
567 during the last four centuries. Nature GeoSci 2:51–56

568 Douglass AE (1920) Evidence of climate effects in the annual rings of trees. Ecology 1:24–32

569 Driscoll S, Bozzo A, Gray LJ, Robock A, Stenchikov G (2012) Coupled Model
570 Intercomparison Project 5 (CMIP5) simulations of climate following volcanic eruptions. J
571 Geophys Res 117. doi:10.1029/2012JD017607

572 Esper J, Cook ER, Schweingruber FH (2002) Low-frequency signals in long tree-ring
573 chronologies and the reconstruction of past temperature variability. Science 295:2250–2253

574 Esper J, Frank DC, Wilson RJS, Briffa KR (2005) Effect of scaling and regression on
575 reconstructed temperature amplitude for the past millennium. Geophys Res Lett 32.
576 doi:10.1029/2004GL021236

577 Esper J, Büntgen U, Frank DC, Nievergelt D, Liebhold A (2007a) 1200 years of regular
578 outbreaks in alpine insects. Proceed Royal Soc B 274:671–679

579 Esper J, Büntgen U, Frank D, Pichler T, Nicolussi K (2007b) Updating the Tyrol tree- ring
580 dataset. In: Haneca K, et al. (eds), Tree rings in archaeology, climatology and ecology.
581 TRACE 5:80–85

582 Esper J, Frank DC, Büntgen U, Verstege A, Hantemirov RM, Kirdyanov AV (2010) Trends
583 and uncertainties in Siberian indicators of 20th century warming. Glob Change Biol 16:386–
584 398

585 Esper J, Büntgen U, Timonen M, Frank DC (2012a) Variability and extremes of Northern
586 Scandinavian summer temperatures over the past millennia. Glob Plan Change 88-89:1–9

587 Esper J, Frank DC, Timonen M, Zorita E, Wilson RJS, Luterbacher J, Holzkämper S, Fischer
588 N, Wagner S, Nievergelt D, Verstege A, Büntgen U (2012b) Orbital forcing of tree-ring data.
589 Nature Clim Change 2:862–866

590 Esper J, Büntgen U, Luterbacher J, Krusic P (2013) Testing the hypothesis of post-volcanic
591 missing rings in temperature sensitive dendrochronological data. Dendrochronologia,
592 http://dx.doi.org/10.1016/j.dendro.2012.11.002

593 Farquhar, GD, Roderick ML (2003) Pinatubo, diffuse light, and the carbon cycle, Science
594 299:1997–1998

595 Fernández-Donado L, et al. (2013) Large-scale temperature response to external forcing in
596 simulations and 50 reconstructions of the last millennium. Clim Past 9:393–421

597 Fischer EM, Luterbacher J, Zorita E, Tett FB, Casty C, Wanner H (2007) European climate
598 response to tropical volcanic eruptions over the last half millennium. Geophys Res Lett 34,
599 L05707. doi:10.1029/2006GL027992

600 Frank D, Büntgen U, Böhm R, Maugeri M, Esper J (2007) Warmer early instrumental
601 measurements versus colder reconstructed temperatures: shooting at a moving target. Quat Sc
602 Rev 26:3298-3310

603 Frank D, Esper J, Zorita E, Wilson RJS (2010) A noodle, hockey stick, and spaghetti plate: a
604 perspective on high-resolution paleoclimatology. WIREs Clim Change 1:507–516

605 Gao C, et al. (2006) The 1452 or 1453 A.D. Kuwae eruption signal derived from multiple ice
606 core records: Greatest volcanic sulfate event of the past 700 years. J Geophys Res 111.
607 doi:10.1029/2005JD006710

608 Gao C, Robock A, Ammann C (2008) Volcanic forcing of climate over the past 1500 years:
609 An improved ice core-based index for climate models. J Geophys Res 113 D23111.
610 doi:10.1029/2008JD010239

611 Gent PR., et al. (2011) The Community Climate System Model Version 4. J Climate
612 24:4973–4991

613 Gleckler PJ, AchutaRao K, Gregory JM, Santer BD, Taylor KE, Wigley TML (2006)
614 Krakatoa lives: the effect of volcanic eruptions on ocean heat content and thermal expansion.
615 Geophys Res Lett 33. doi:10.1029/2006GL026771

616 Graham NE et al. (2007) tropical Pacific – mid-latitude teleconnections in medieval times.
617 Clim Change 83:241–285

618 Graham NE, Ammann CM, Fleitmann D, Cobb KM, Luterbacher J (2011) Support for global
619 climate reorganization during the "Medieval Climate Anomaly. Clim Dyn 37:1217–1245

620 Grove JM (2001) The initiation of the ‘‘Little Ice Age’’ in regions round the North Atlantic.
621 Clim Change 48:53–82

622 Grudd H (2008) Tornetraesk tree-ring width and density AD 500–2004: a test of climatic
623 sensitivity and a new 1500-year reconstruction of north Fennoscandian summers. Clim Dyn
624 31:843–857

625 Gunnarson BE, Linderholm HW, Moberg A (2010) Improving a tree-ring reconstruction from
626 west-central Scandinavia – 900 years of warm-season temperatures. Clim Dyn.
627 doi:10.1007/s00382-010-0783-5

628 Hammer CU, Clausen HB, Dansgaard W (1980) Greenland ice sheet evidence of post-glacial
629 volcanism and its climatic impact. Nature 288:230–235

630 Hammer CU, Clausen HB, Tauber H (1986) Ice-cored dating of the Pleistocene/Holocene
631 boundary applied to a calibration of the ^{14}C timescale. Radiocarbon 28: 284-291

632 Hegerl GC, Crowley TS, Baum SK, Kim K-Y, Hyde WT (2003) Detection of volcanic, solar
633 and greenhouse gas signals in paleo-reconstructions of Northern Hemispheric temperature.
634 Geophys Res Lett 30. doi:10.1029/2002GL016635

635 Hegerl G, Luterbacher J, González-Rouco F, Tett SFB, Crowley TJ, Xoplaki E (2011)
636 Influence of human and natural forcing on European seasonal temperatures. Nat Geosci 4:99–
637 103

638 Jones PD, Moberg A, Osborn TJ, Briffa KR (2003) Surface climate responses to explosive
639 volcanic eruptions seen in long European temperature records and mid-to-high latitude tree-
640 ring density around the Northern Hemisphere. Geophys Monogr Ser 139:239–254

641 Jones PD, Lister DH, Osborn TJ, Harpham C, Salmon M, Morice CP (2012) Hemispheric and
642 large-scale land surface air temperature variations: an extensive revision and an update to
643 2010. J Geophys Res 117 D05127. doi:10.1029/2011JD017139

644 Jungclaus JH, et al. (2010) Climate and carbon-cycle variability over the last millennium.
645 Clim Past 6:723–737

646 Kelly PM, Sear CB (1984) Climatic impact of explosive volcanic eruptions. Nature 311:740–
647 743

648 Krakauer NY, Randerson JT (2003) Do volcanic eruptions enhance or diminish net primary
649 production? Evidence from tree rings. Glob Biogeochem Cycl 17.
650 doi:10.1029/2003GB002076

651 Kurbatov AV, Zielinski GA, Dunbar NW, Mayewski PA, Meyerson EA, Sneed SB, Taylor
652 KC (2006) A 12,000 year record of explosive volcanism in the Siple Dome Ice Core, West
653 Antarctica. J Geophys Res 111 D12307. doi:10.1029/2005JD006072

654 LaMarche VC, Hirschboeck KK (1984) Frost rings in trees as records of major volcanic
655 eruptions. Nature 307:121–126

656 Langway CC, Clausen HB, Hammer CU (1988) An inter-hemispheric volcanic time-marker
657 in cores from Greenland and Antarctica. Ann Glaciol 10:102–108

658 Mann ME, Fuentes JD, Rutherford S (2012) Underestimation of volcanic cooling in tree-ring-
659 based reconstructions of hemispheric temperatures. Nature Geosc 5:202–205

660 Mass CF, Portman DA (1989) Major volcanic eruptions and climate: a critical evaluation. J
661 Clim 2:566–593

662 McCormick PM, Wang PH, Poole LR (1993) Stratospheric aerosols and clouds. In: Hobbs
663 PV (ed) Aerosol-cloud-climate interactions. Academic Press, San Diego, pp 205–222

664 Miller, GH et al. (2012) Abrupt onset of the Little Ice Age triggered by volcanism and
665 sustained by sea-ice/ocean feedbacks. Geophys Res Lett 39 L02708. doi:10.1029/
666 2011GL050168

667 Moser L, Fonti P, Büntgen U, Esper J, Luterbacher J, Franzen J, Frank D (2010) Timing and
668 duration of European larch growing season along an altitudinal gradient in the Swiss Alps.
669 Tree Physiol 30:225–233

670 Mitchell TM, Jones PD (2005) An improved method of constructing a database of monthly
671 climate observations and associated high-resolution grids. Int J Climatol 25:693–712

672 Newhall CG, Self S (1982) The volcanic explosivity index (VEI): an estimate of explosive
673 magnitude for historical volcanism. J Geophys Res 87:1231–1238

674 Oppenheimer C (2003) Ice core and palaeoclimatic evidence for the timing and nature of the
675 great mid-13th century volcanic eruptions. Int J Climatol 23:417–426

676 Panofsky HA, Brier GW (1958) Some applications of statistics to meteorology. Univ. Park,
677 Pennsylvania.

678 Plummer CT, et al. (2012) An independently dated 2000-yr volcanic record from Law Dome,
679 East Antarctica, including a new perspective on the dating of the c. 1450s eruption of Kuwae,
680 Vanuatu. Clim Past Discuss 8:1567–1590

681 Robock A, Free MP (1995) Ice cores as an index of global volcanism from 1850 to the
682 present. J Geophys Res 100:11549-11567

683 Robock A, Mao J (1995) The volcanic signal in surface temperature observations. J Clim
684 8:1086–1103

685 Robock A (2000) Volcanic eruptions and climate. Rev Geophys 38:191–219

686 Salzer MW, Hughes MK (2007) Bristlecone pine tree rings and volcanic eruptions over the
687 last 5000 yr. Quat Res 2007, 67:57–68

688 Schneider DP, Ammann CM, Otto-Bliesner BL, Kaufman DS (2009) Climate response to
689 large, high-latitude and low-latitude volcanic eruptions in the Community Climate System
690 Model. J Geophys Res 114 D15101. doi:10.1029/2008JD011222

691 Schweingruber FH, Fritts HC, Bräker OU, Drew, LG, Schaer E (1978) The X-ray technique
692 as applied to dendroclimatology. Tree-Ring Bull 38:61–91

693 Schweingruber FH, Bartholin T, Schär E, Briffa KR (1988) Radiodensitometric–
694 dendroclimatological conifer chronologies from Lapland (Scandinavia) and the Alps
695 (Switzerland). Boreas 17:559–566

696 Sear CB, Kelly PM, Jones PD, Goodess CM (1987), Global surface temperatures responses to
697 major volcanic eruptions, Nature 330:365–367

698 Self S, Rampino MR, Barbera JJ (1981) The possible effects of large 19th and 20th century
699 volcanic eruptions on zonal and hemispheric surface temperatures. J Vol Geothermal Res
700 11:41–60

701 Sigl M, et al. (2012) A new bipolar ice core record of volcanism from WAIS Divide and
702 NEEM and implications for climate forcing of the last 2000 years J Geophys Res
703 doi:10.1029/2012JD018603, in press

704 Plummer CT, et al. (2012) An independently dated 2000-yr volcanic record from Law Dome,
705 East Antarctica, including a new perspective on the dating of the c. 1450s eruption of Kuwae,
706 Vanuatu. Clim Past Discuss 8:1567–1590

707 Siebert L, Simkin T, Kimberly P (2010) Volcanoes of the world. Univ. California Press,
708 London

709 Solomon S, Qin D, Manning M, Chen Z, Marquis M, Averyt KB, Tignor M, Miller HL (eds)
710 (2007) Climate change 2007: the physical science basis. Contribution of working group I to

711 the fourth assessment report of the Intergovernmental Panel on Climate Change. Cambridge
712 Univ Press, Cambridge

713 Stenchikov G, Hamilton K, Stouffer RJ, Robock A, Ramaswamy V, Santer B, Graf HF
714 (2006) Arctic Oscillation response to volcanic eruptions in the IPCC AR4 climate models. J
715 Geophys Res 111. doi:10.1029/2005JD006286

716 Stothers RB (1984) The great Tambora eruption in 1815 and its aftermath. Science 224:1191–
717 1198

718 Taylor KE, Stouffer RJ, Meehl GA (2012) An overview of CMIP5 and the experimental
719 design. Bull Amer Meteor Soc 93:485-497

720 Timmreck C, Lorenz SJ, Crowley TJ, Kinne S, Raddatz TJ, Thomas MA, Jungclaus JH
721 (2009) Limited temperature response to the very large AD 1258 volcanic eruption. Geophys
722 Res Lett 36. doi:10.1029/2009GL040083

723 Traufetter F, Oerter H, Fischer H, Weller R, Miller H (2004) Spatio-temporal variability in
724 volcanic sulphate deposition over the past 2 kyrs in snow pits and firn cores from
725 Amundsenisen, Antarctica. Claciol 50:137–146

726 Trepte CR, Hitchman MH (1992) tropical stratospheric circulation deduced from satellite
727 aerosol data. Nature 355:626–628

728 Trouet V, Esper J, Graham NE, Baker A, Scourse JD, Frank DC (2009) Persistent positive
729 North Atlantic Oscillation mode dominated the Medieval Climate Anomaly. Science 324:78–
730 80

731 Wagner S, Zorita E (2005) The influence of volcanic, solar and CO2 forcing on the
732 temperatures in the Dalton Minimum (1790–1830): a model study. Clim Dyn 25:205-218

733 Zanchettin D, Timmreck C, Bothe O, Lorenz S, Hegerl G, Graf H-F, Luterbacher J,
734 Jungclaus, JH (2013a) Delayed winter warming: a decadal dynamical response to strong
735 tropical volcanic eruptions. Geophys Res Lett 40:204–209

736 Zanchettin D, Bothe O, Graf H-F, Luterbacher J, Jungclaus JH, Timmreck C (2013b)
737 Background conditions influence decadal climate response to strong volcanic eruptions. J
738 Geophys Res. doi:10.1002/jgrd.50229

739 Zielinski GA (1995) Stratospheric loading and optical depth estimates of explosive volcanism
740 over the last 2100 years derived from the Greenland Ice Sheet Project 2 ice core. J Geophys
741 Res 100:20937–20955

742 Zorita E, Gonzlez-Rouco F, von Storch H, Montavez JP, Valero F (2005) Natural and
743 anthropogenic modes of surface temperature variations in the last thousand years. Geophys
744 Res Lett 32 L08707. doi:10.1029/2004GL021563

745

Table and Figure Captions

Table 1 Volcanic eruptions. The 34 annually dated and documented volcanic eruptions (VEI index ≥ 5) in the NH extratropics and tropics from 1111-1976 C.E. SEAs 2-7 indicate subsets of events used to estimate JJA temperature responses in European MXD chronologies. Bottom two lines summarize the temperature response in the second post-eruption year in Northern Europe and the first post-eruption year in Central Europe

Table 2 European MXD chronologies. Period refers to the time span during which replication exceeds two MXD measurement series (-181 denotes 181 B.C.). Mean replication is the average number of MXD measurement series over the 1111-1976 C.E. common period. Lag 1 autocorrelation is calculated for the NegExp detrended chronologies over the same period. MXD-north and MXD-central are the mean timeseries of the three MXD site chronologies from Northern Europe (JAE, TOR, NSC) and the four MXD site chronologies in Central Europe (PYR, LAU, LOE, TIR)

Table 3 JJA temperature signals of European MXD chronologies. Pearson correlation coefficients of the MXD site and regional mean chronologies with JJA temperatures of the nearest grid points from the Crutem4 dataset (Jones et al. 2012) over the 1901-1976 period, together with the correlations with JJA mean temperatures of the long station records in Northern Europe (Uppsala and Stockholm) and Central Europe (Central England, De Bilt, and Berlin) over the 1722-1976 period

Fig. 1 NSC maximum latewood density data. **a** NegExp detrended single MXD measurement series (black) shown together with their bi-weighted robust mean (red) over the 1111-1976 C.E. period. **b** and **c**, Same as in **a**, but shown over the earliest (1111-1140 C.E.) and latest (1947-1976 C.E.) 30-year periods

Fig. 2 European maximum latewood density records. MXD site chronologies (black) from **a** Northern (JAE, TOR, NSC) and **b** Central Europe (PYR, LAU, LOE, TIR) over their common period 1111-1976 C.E. Records were smoothed using a 30-year filter. Blue and red curves are the regional mean timeseries derived from averaging the unsmoothed site records in Northern (blue) and Central Europe (red) respectively. The years of the four most negative deviations are labeled. **c** Temporal sample depth of all MXD measurement series (stem radii) within each site chronology in Northern (bluish colors) and Central Europe (reddish colors). The well-replicated site chronologies in Northern (NSC) and Central Europe (PYR, LOE) are labeled. **d** 100-year running inter-site correlations among the three northern (blue) and central site chronologies (red), and between the northern and central regional records (grey)

779 **Fig. 3** MXD temperature signals. Maps showing the correlation patterns of MXD site
780 chronologies (red dots) with gridded JJA mean temperatures (Mitchell and Jones 2005) over
781 the common 1901-1976 period ($p < 5\%$). Bottom panels indicate the results for the regional
782 mean timeseries, MXD-north and MXD-central

783 **Fig. 4** Superposed Epoch Analyses centered on large volcanic eruptions of the past nine
784 centuries. **a** JJA temperature patterns of MXD-north (blue) and MXD-central (red) five years
785 before and after the 34 large volcanic eruptions (VEI index ≥ 5) within the 1111-1976 C.E.
786 period (SEA1 in Table 1). Thin curves are the SEA timeseries of the individual MXD site
787 records JAE, TOR, and NSC in Northern Europe, and PYR, LAU, LOE, and TIR in Central
788 Europe. **b** Same as in **a**, but for the 15 eruptions of the 1722-1976 C.E. period (SEA2). **c**,
789 Same as in **b**, but using the JJA instrumental temperatures (instead of the MXD-derived
790 estimates). **d** and **e**, Same as in **a**, but for the 21 eruptions located in the NH extratropics and
791 13 eruptions in the (NH and SH) tropics, respectively. All SEA timeseries expressed as
792 temperature anomalies with respect to the five years preceding the volcanic events (lags -5 to
793 -1)

794 **Fig. 5** Summarized SEA results for stratospheric volcanic events at lag 0, +1, and +2 in the
795 MXD-north (blue), MXD-central (red), JJA-north (light blue), and JJA-central (light red)
796 datasets

797 **Fig. 6** Distributions of reconstructed and recorded JJA temperatures over the 1111-1976 and
798 1722-1976 C.E. periods. Left column shows temperatures in Northern Europe two years after
799 volcanic eruptions (SEA1: lag +2), right column shows temperatures in Central Europe one
800 year after volcanic eruptions (SEA1: lag +1). Green curves indicate density functions
801 (bandwidth = 0.3) of JJA temperature anomalies with respect to the 1111-1976 and 1722-
802 1976 periods (thin grey and red lines; 866 years in the top panels, 255 years in the middle and
803 bottom panels). Red lines indicate summer temperatures in 34 post-volcanic years (lag +2 in
804 the left, and lag +1 in the right column). Bold red lines and triangles indicate the mean
805 temperature of these lag years. Bold black lines and triangles indicate the mean temperature
806 of all years. Results are for MXD-based (top and middle panels) and observational (bottom
807 panels) JJA temperatures

Table 1

						Superposed Epoch Analyses (SEA)						
Year	**Season**	**Volcano and Region**	**VEI***	**Lat.**	**Tephra†**	**Long period (SEA1)**	**Short period (SEA2)**	**Large events (SEA3)**	**Small events (SEA4)**	**Extra-tropics (SEA5)**	**Tropics (SEA6)**	**Gao08 (NH)** (SEA7)**
1262	?	Katla (Iceland)	5	64°N	1.5	✓		✓		✓		
1362	2	Oraefajokull (Iceland)	5	64°N	2.3	✓		✓		✓		
1471	4	Sakura-Jima (Japan)	5?	32°N	1.3	✓			✓	✓		
1477	1?	Bardarbunga (Iceland)	6	65°N	10	✓		✓		✓		
1563	2	Agua de Pau (Azores)	5?	38°N	1	✓			✓	✓		
1586	?	Kelut (Indonesia)	5?	8°S	1	✓			✓		✓	
1593	?	Raung (Indonesia)	5?	8°S	1	✓			✓		✓	
1600	1	Huaynaputina (Peru)	6	17°S	30	✓		✓			✓	✓
1625	3	Katla (Iceland)	5	64°N	1.5	✓		✓		✓		
1630	3	Furnas (Azores)	5	38°N	2.1	✓		✓		✓		
1631	4	Vesuvius (Italy)	5?	41°N	1.1	✓			✓	✓		
1640	3	Komaga-Take (Japan)	5	42°N	2.9	✓		✓		✓		
1641	1	Parker (Philippines)	5?	6°N	1	✓			✓		✓	✓
1663	3	Usu (Japan)	5	43°N	2.8	✓		✓		✓		
1667	3	Shikotsu (Japan)	5	43°N	3.4	✓		✓		✓		
1673	2	Gamkonora (Indonesia)	5?	1°N	1	✓			✓		✓	✓
1680	?	Tongkoko (Indonesia)	5?	2°N	1	✓			✓		✓	
1707	4	Fuji (Japan)	5	35°N	2.1	✓		✓		✓		
1721	2	Katla (Iceland)	5?	64°N	1.2	✓			✓	✓		
1739	3	Shikotsu (Japan)	5	43°N	4	✓	✓	✓		✓		
1755	4	Katla (Iceland)	5?	63°N	1.5	✓	✓	✓		✓		✓
1815	2	Tambora (Indonesia)	7	8°S	160	✓	✓	✓			✓	✓
1822	4	Galunggung (Indonesia)	5	7°S	1	✓	✓		✓		✓	
1835	1	Cosiguina (Nicaragua)	5	13°N	5.7	✓	✓	✓			✓	✓
1854	1	Shiveluch (Russia)	5	56°N	2	✓	✓	✓		✓		
1875	1	Askja (Iceland)	5	65°N	1.8	✓	✓	✓		✓		
1883	3	Krakatau (Indonesia)	6	6°S	20	✓	✓	✓			✓	✓
1902	4	Santa Maria (Guatemala)	6?	15°N	20	✓	✓	✓			✓	
1907	2?	Ksudach (Russia)	5	52°N	2.8	✓	✓	✓		✓		
1912	2	Novarupta (USA)	6	58°N	28	✓	✓	✓		✓		✓
1913	1	Colima (Mexico)	5	19°N	1.7	✓	✓	✓			✓	
1933	1	Kharimkotan (Kuril Isl.)	5	49°N	1	✓	✓		✓	✓		
1956	1	Bezymianny (Russia)	5	56°N	2.8	✓	✓	✓		✓		
1963	1	Agung (Indonesia)	5	8°S	1	✓	✓		✓		✓	✓
					Number of events	34	15	22	12	21	13	9
					Mean tephra vol. (billion m3)	9.4	16.9	14.0	1.1	3.7	18.8	(23.2)§
			JJA temperature response		MXD-north (lag +2)	-0.52	-0.65	-0.46	-0.61	-0.41	-0.68	-0.15
					MXD-central (lag +1)	-0.18	-0.29	-0.17	-0.19	-0.01	-0.44	-0.18

*Volcanic explosivity index. (?) indicates uncertain assignments.

†Estimated volume in billion m^3.

**Ice core derived volcanic sulfate deposition signals from Gao et al. (2008). 9 of the total of 40 NH volcanic events reconstructed in Gao et al. (2008) for the 1111-1976 period match the VEI≥4 events listed here. All 40 NH deposition events were used in the SEA.

§Mean NH stratospheric sulfate aerosol injection (in Tg) according to Gao et al. 2008.

Table 2

MXD Chronoloy	Country	Species	Period	Mean replication (1111-1976)	Lag 1 auto-correlation	Source
Jaemtland (JAE)	Sweden	Pine	1111-1978	29	0.12	Gunnarson et al. 2010
Tornetraesk (TOR)	Sweden	Pine	452-2004	18	0.17	Grudd 2008
N-Scan (NSC)	Finland	Pine	-181–2006	49	0.25	Esper et al. 2012
MXD-north			*1111–1976*	*96*	*0.18*	
Pyrenees (PYR)	Spain	Pine	1044-2005	46	0.00	Büntgen et al. 2008
Lauenen (LAU)	Switzerland	Spruce	996-1976	22	0.03	Schweingruber et al. 1988
Lötschental (LOE)	Switzerland	Larch	743-2004	46	0.37	Büntgen et al. 2006
Tirol (TIR)	Austria	Spruce	1047-2003	33	0.07	Esper et al. 2007
MXD-central			*1111-1976*	*147*	*0.10*	

Table 3

MXD Chronoloy	Crutem4 grid point	Correlation with Crutem4 (1901-1976)	Correlation with long station record (1722-1976)
JAE	67.5°N/12.5°E	0.71	0.59
TOR	67.5°N/22.5°E	0.82	0.56
NSC	67.5°N/22.5°E	0.76	0.52
MXD-north	*mean*	*0.80*	*0.61*
PYR	42.5°N/2.5°E	0.40	0.17
LAU	47.5°N/7.5°E	0.31	0.29
LOE	47.5°N/7.5°E	0.61	0.42
TIR	47.5°N/12.5°E	0.41	0.27
MXD-central	*mean*	*0.52*	*0.36*

Figure 1

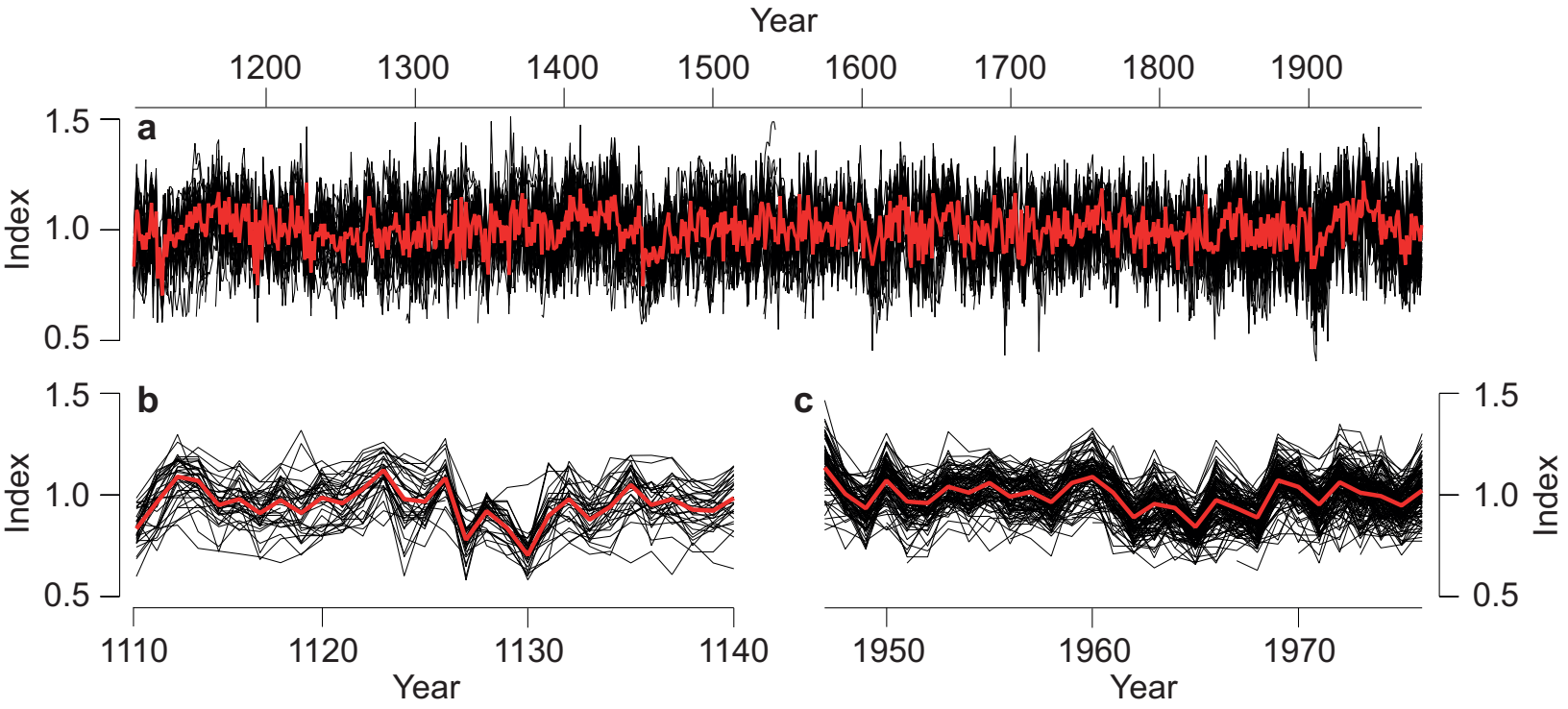
Year
1200
1300
1400
1500
1600
1700
1800
1900
a
Index
1.5
1.0
0.5
b
c
1110
1120
1130
1140
1950
1960
1970
Year

Figure 2

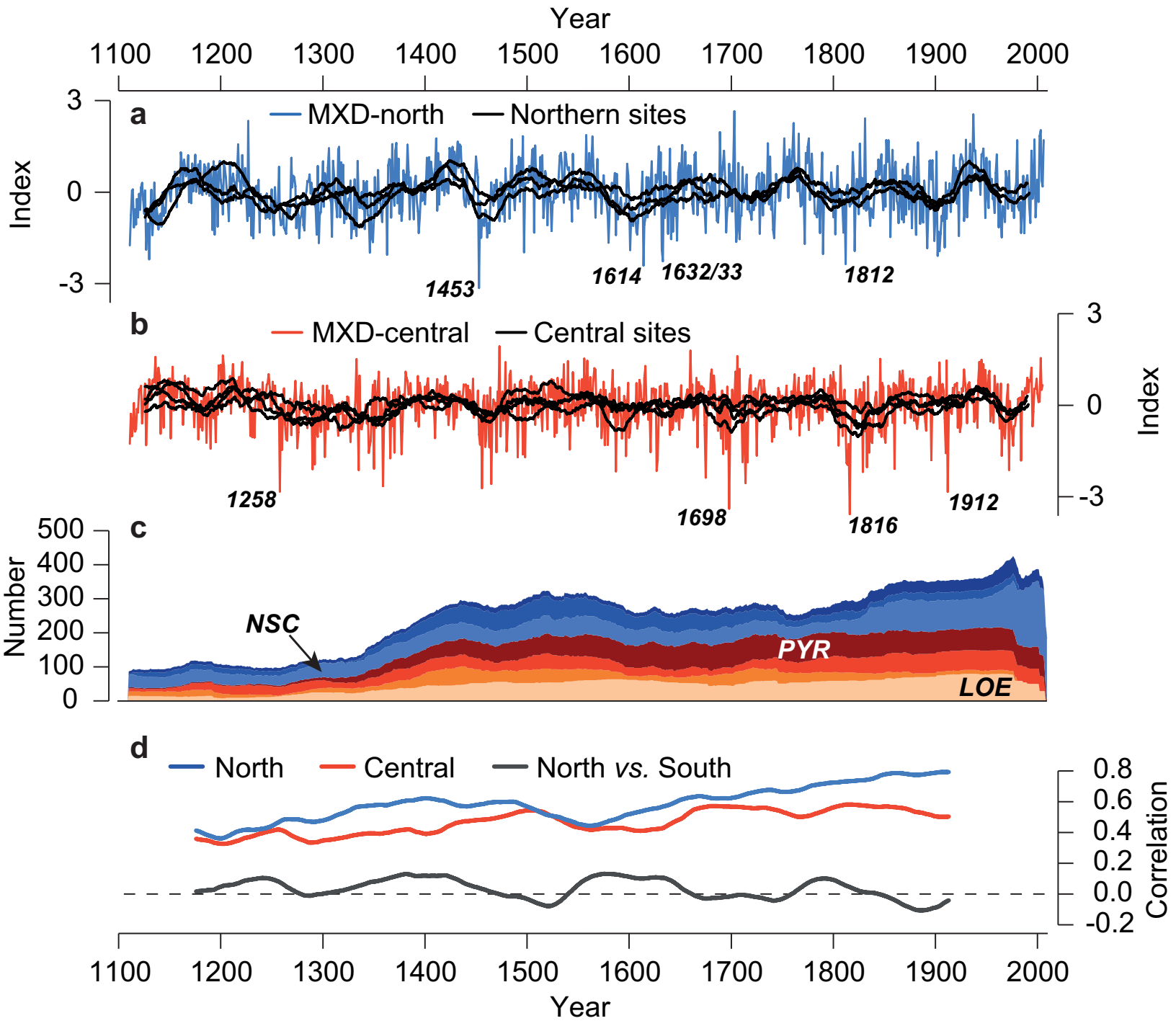
Year
1100
1200
1300
1400
1500
1600
1700
1800
1900
2000
a
MXD-north
Northern sites
Index
3
0
-3
1453
1614
1632/33
1812
b
MXD-central
Central sites
1258
1698
1816
1912
Index
3
0
-3
c
Number
500
400
300
200
100
0
NSC
PYR
LOE
d
North
Central
North vs. South
0.8
0.6
0.4
0.2
0.0
-0.2
Correlation
1100
1200
1300
1400
1500
1600
1700
1800
1900
2000
Year

Figure 3

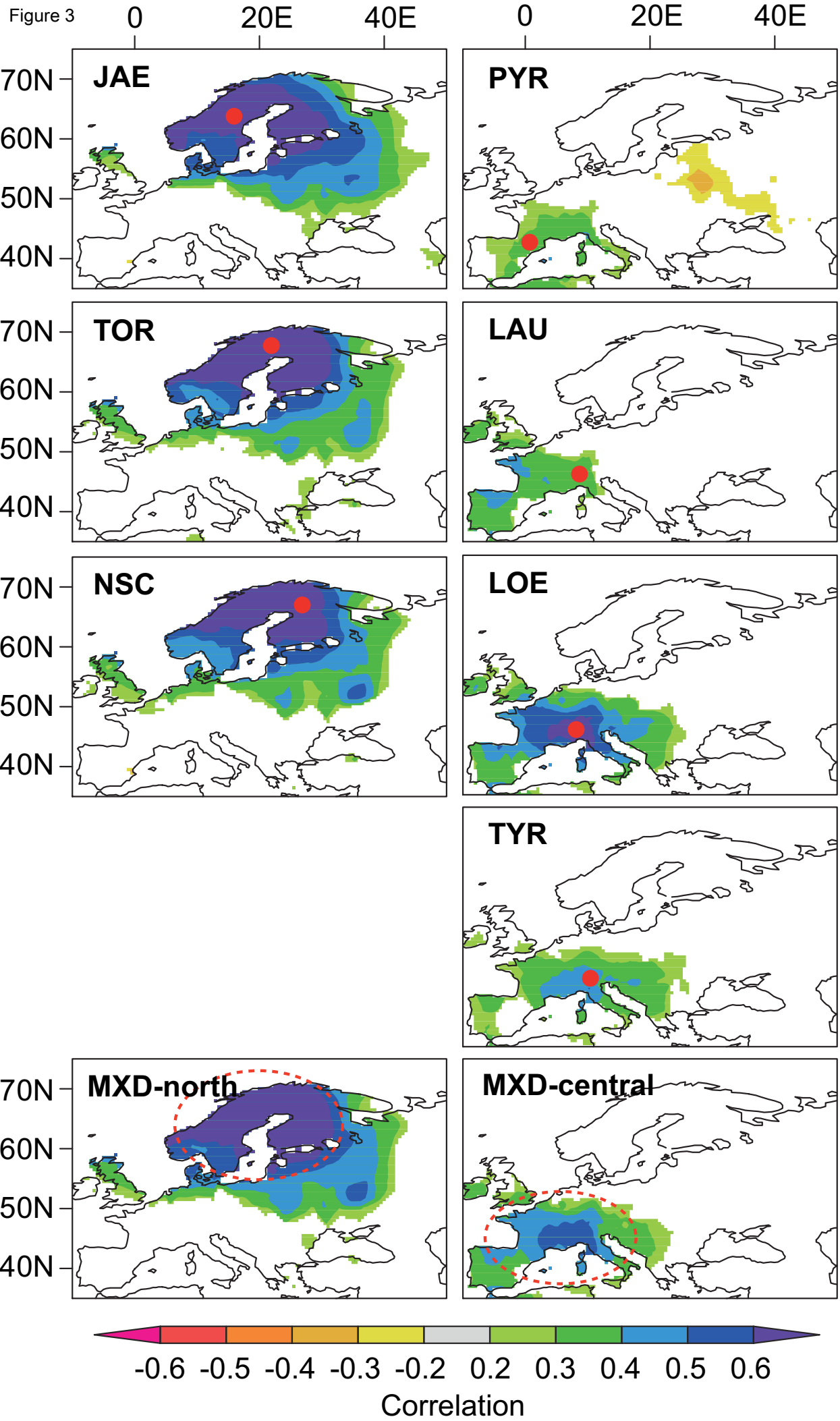
0
20E
40E
70N
60N
50N
40N
JAE
PYR
TOR
LAU
NSC
LOE
TYR
MXD-north
MXD-central
-0.6 -0.5 -0.4 -0.3 -0.2 0.2 0.3 0.4 0.5 0.6
Correlation

Figure 4

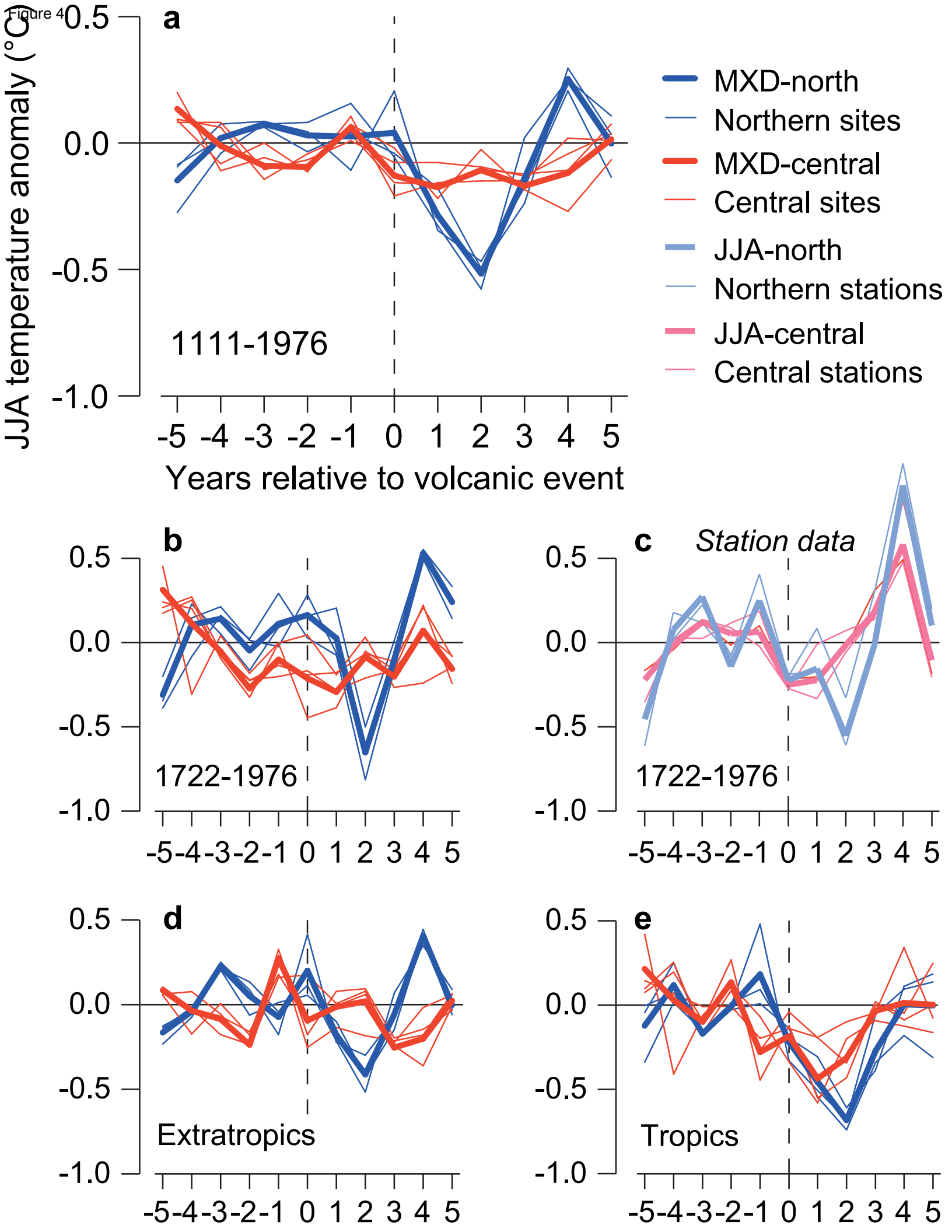
a
JJA temperature anomaly (°C)
0.5
0.0
-0.5
-1.0
1111-1976
-5 -4 -3 -2 -1 0 1 2 3 4 5
Years relative to volcanic event
MXD-north
Northern sites
MXD-central
Central sites
JJA-north
Northern stations
JJA-central
Central stations
b
1722-1976
c
Station data
1722-1976
d
Extratropics
e
Tropics

Figure 5

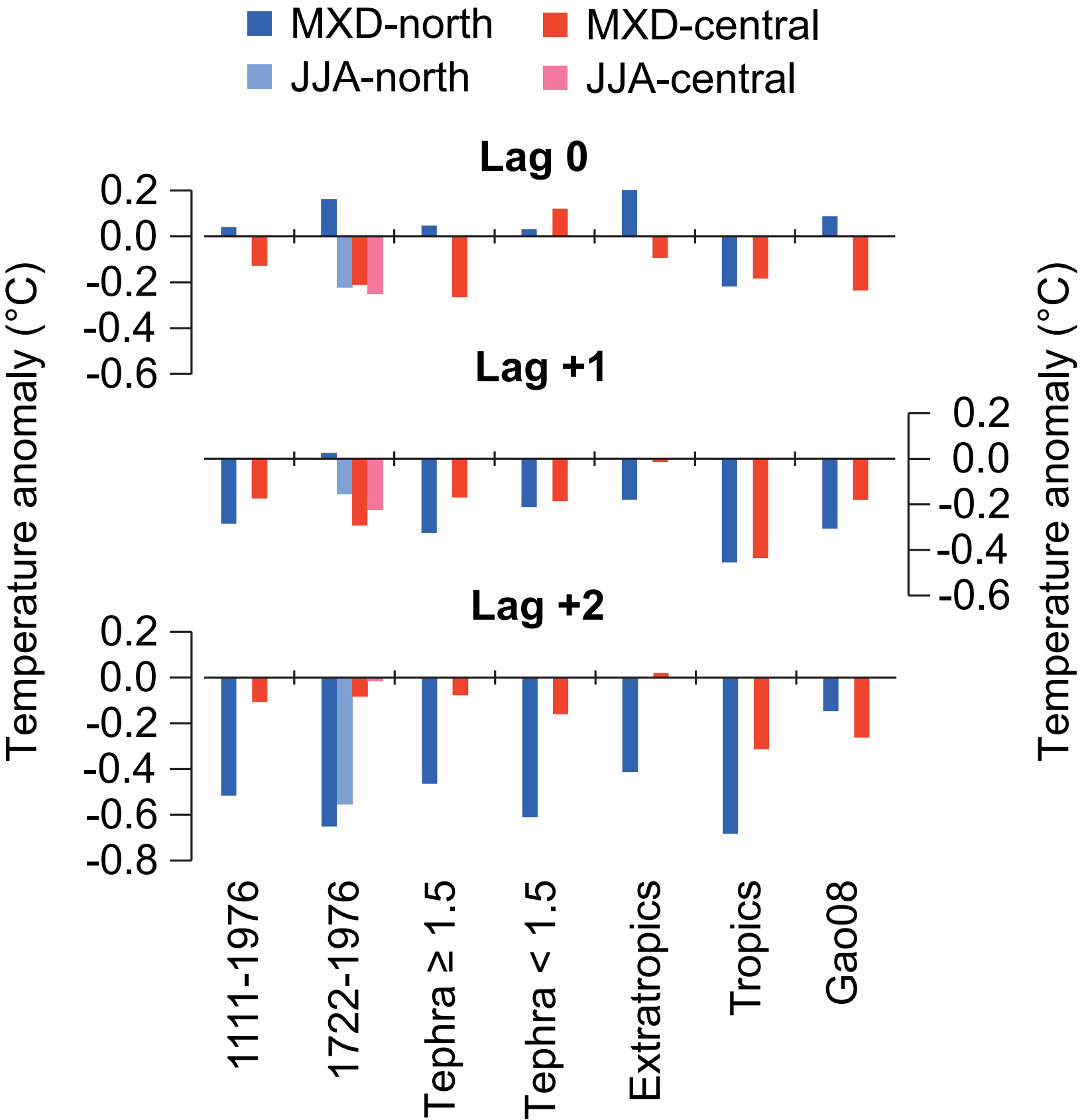
MXD-north
MXD-central
JJA-north
JJA-central
Lag 0
Lag +1
Lag +2
Temperature anomaly (°C)
0.2
0.0
-0.2
-0.4
-0.6
-0.8
1111-1976
1722-1976
Tephra ≥ 1.5
Tephra < 1.5
Extratropics
Tropics
Gao08

Figure 6

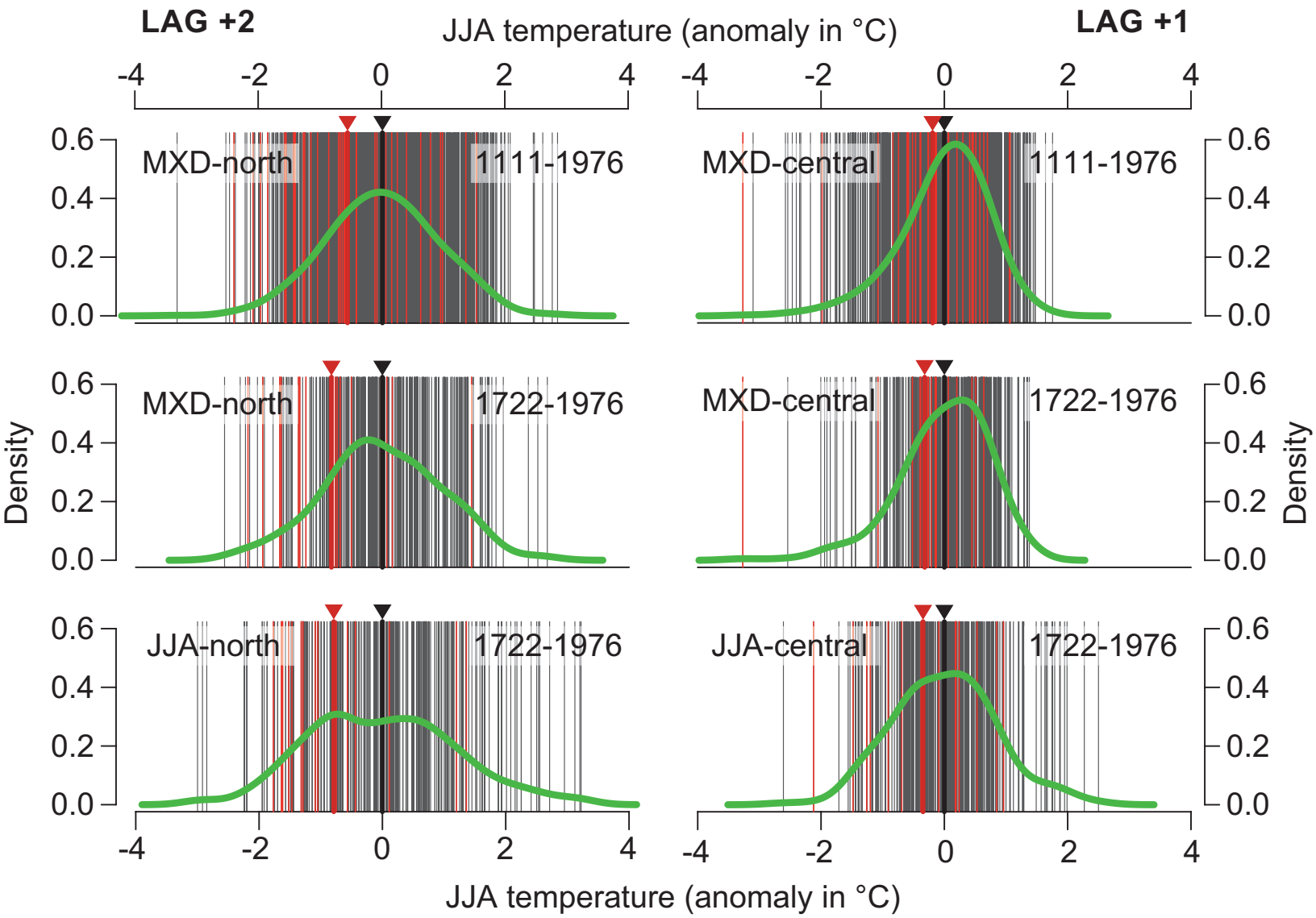
LAG +2
JJA temperature (anomaly in °C)
LAG +1
-4
-2
0
2
4
MXD-north
1111-1976
MXD-central
1111-1976
MXD-north
1722-1976
MXD-central
1722-1976
JJA-north
1722-1976
JJA-central
1722-1976
0.6
0.4
0.2
0.0
Density
JJA temperature (anomaly in °C)

Supplementary Material

Click here to download Supplementary Material: esper_supplement.docx